



# Spatial early warning signals for tipping points using dynamic mode decomposition

G.M. Donovan <sup>\*</sup>, C. Brand

Department of Mathematics, University of Auckland, Private Bag 9201, Auckland 1142, New Zealand

## ARTICLE INFO

### Article history:

Received 10 August 2021

Received in revised form 20 February 2022

Available online 28 February 2022

### Keywords:

Tipping points

Leading indicator

Early warning signal

Critical slowing down

Dynamic mode decomposition

## ABSTRACT

Tipping points are abrupt transitions in time-varying systems which may be driven by noise, changes in the underlying system, or some combination of the two. Early warning signals of tipping points are potentially valuable leading indicators of these transitions. In low-dimensional systems, it is possible to characterize these indicators based on the expected type of the tipping point. In spatial systems, indicators which take account of changes in the spatial structure are in principle able to capture more information, compared with aggregate measures, and thus provide stronger leading indicators. Here we propose the use of *dynamic mode decomposition* (DMD), a dimensionality reduction technique first developed in a fluid dynamics context, as a method for extracting useful information about critical slowing down in the leading mode of a spatial system approaching a tipping point. To demonstrate its potential utility for this purpose we employ two models: one drawn from the physiology literature for the study of spatially-patterned ventilation distributions in asthma, and the other an ecological model previously used for the study of spatial early warning signals of tipping points. Together these show that the DMD leading eigenvalue may be a useful spatially-informed early warning signal.

© 2022 Elsevier B.V. All rights reserved.

## 1. Introduction

Tipping points, defined as abrupt transitions in time-varying systems, have generated much interest in climate and ecology for their potential to predict, understand and/or mitigate phenomena such as climate change and ecosystem collapse (e.g. [1]). Other areas, such as physiology [2], have similar concepts in disease exacerbations, though perhaps without the same level of interest to date. Tipping points are often classified as [3]

- Bifurcation-driven tipping, or *B-tipping*, in which the equilibria of the underlying system change qualitatively;
- Noise-driven tipping, or *N-tipping*, in which the system transitions between stable equilibria, driven by noise; or
- Rate-driven tipping, or *R-tipping*, in which the system is unable to track the quantitative changes of the current equilibrium.

Within these broad categories, further distinctions can be made; for example, B-tipping analysis may be further broken down by classification of the bifurcations involved [4]. Much current research is dedicated to the subtleties of R-tipping.

<sup>\*</sup> Corresponding author.

E-mail address: [g.donovan@auckland.ac.nz](mailto:g.donovan@auckland.ac.nz) (G.M. Donovan).

URL: <https://www.math.auckland.ac.nz/~gdon030/> (G.M. Donovan).

An obvious area of interest is anticipating tipping points by way of so-called *early warning signals* (EWS). One example is the phenomenon known as *critical slowing down* [5,6], in which, as the tipping point is approached, the system becomes slower to return to equilibrium after perturbation. This can be indicated by changes in the variance or autocorrelation of the time series of system observations. Many other EWS indicators have also been proposed [7].

All of the above applies in the context of analysis of time series signals; imagine, for example, mean surface temperature in a climate context, or species population numbers in an ecological one. However, many systems of interest are spatial systems. If we have information about the spatial distribution of the system (vegetation patterns, for instance), does this encode useful information about tipping points and early warning signals? Naively, spatially-informed indicators may be more valuable for these systems, compared with aggregate measures, because they take account of this spatial structure.

Intuitively we expect that spatial analysis will be useful for systems which exhibit patterns or other spatial structure – by analysing only aggregate measures we are discarding potentially useful information. Following this line of thinking, several spatial measures, such as spatial correlation [8], variance, skewness [9] and the discrete Fourier transform [10] have been proposed [11,12]. Although the theory of spatial EWS is much less developed than their non-spatial, low-dimensional cousins, at least in a B-tipping context there is reason to expect spatial changes which reflect critical slowing down in the leading mode. Chen et al. [13] suggest that one way to capture this slowing down in the leading mode is to do so indirectly, by way of the eigenvalues of the covariance matrix. Here we propose an alternative methodology for spatial EWS: capturing the leading spatial mode more directly using dynamic mode decomposition (DMD).

DMD is a dimensionality reduction technique originally developed in a fluid dynamics context [14] and subsequently applied in many other domains [15,16]. In intuitive terms, it has been described as a combination of principal component analysis (PCA) in space and Fourier analysis in time [17,18], giving a reduced description of both spatial and temporal behaviour [19]. Therefore it is intuitively well-suited to assessing temporal changes in the leading mode. It allows us to capture both the leading spatial mode, and its associated eigenvalue indicating the time variation; in this paper we show that the DMD leading eigenvalue is a promising methodology for use as a spatially-informed EWS of B-tipping.

## 2. Methods

### 2.1. Models

#### 2.1.1. Lung ventilation model

We use as an example system a model drawn from the study of ventilation patterns in asthma [20]. In order to focus on spatial EWS, we employ a simplified version of the original model; the simplifications are summarized in [Appendix](#).

Briefly, the airway dynamics are described in terms of airway luminal radius ( $r$ ) by a continuous-time lattice dynamical system with additive white noise given by

$$\frac{dr_{ij}}{dt} = \left[ 1 + \exp \left( -P_b + \kappa \frac{k}{r_{ij}} + P_b A (r_{ij}^4 + r_{i+1,j}^4 + r_{i-1,j}^4 + \dots + r_{i,j+1}^4 + r_{i,j-1}^4) (1 - r_{ij} + 1.5(1 - r_{ij})^2) + P_l \right) \right]^{-1} - r_{ij} + \sigma dW_{ij} \quad (1)$$

where

$$P_b(t) = \frac{P_b(0)N^2}{\sum_{i,j \in \mathcal{L}} r_{ij}^4} \quad (2)$$

and  $i, j \in \mathcal{L}$  are all lattice elements in the N-by-N square lattice. The nearest-neighbour interactions arise from local expansion of the lung (so-called *parenchymal tethering*) and the global coupling via the assumption that breathing pressures increase to maintain flow despite airway narrowing. The parameter values used are  $P_l = 0.96$ ,  $P_b(0) = 7.25$ ,  $A = 0.63$ , and  $k = 14.1$ , all dimensionless, describing airway compliance and interactions. In broad terms, the simplified, parameters control the strength of breathing ( $P_b(0)$ ), inter-airway coupling via parenchymal interdependence ( $A$ ), airway smooth muscle mass ( $k$ ), and the inflection point of the pressure–radius relationship ( $P_l$ ); more details, and the relationship with the dimensional version of the model, are given in [Appendix](#). The parameter  $\kappa$  describes the degree of smooth muscle activation, which acts to narrow the airways, and is used here as the bifurcation control parameter and assumed to increase linearly with time.

#### 2.1.2. Bifurcation structure of lung ventilation model

The bifurcation structure of the deterministic version of this model (i.e. when  $\sigma = 0$ ) has been previously studied [20]. We will not recapitulate the full analysis here, but several key aspects are relevant to this study. First is that we can locate the bifurcation (with  $\kappa$  as a bifurcation parameter) in which the homogeneous equilibrium loses stability and from which clustered solutions emerge. Writing the system as  $\frac{dr_i}{dt} = f_i(\vec{r})$ , with linear subscript indexing, we express the derivatives evaluated at the homogeneous equilibrium  $r^*$  as

$$\alpha = \left. \frac{\partial f_i}{\partial r_i} \right|_{r=r^*}$$

$$\beta = \left. \frac{\partial f_i}{\partial r_j} \right|_{r=r^*}$$

$$\gamma = \left. \frac{\partial f_i}{\partial r_k} \right|_{r=r^*}$$

for the  $i$ th cell  $r_i$ , where  $r_j$  are the nearest neighbours and  $r_k$  the rest of the cells. Because of the symmetries of the system, the Jacobian of the homogeneous equilibrium then has block circulant structure in terms of  $\alpha$ ,  $\beta$  and  $\gamma$ . Due to this structure, the eigenvalues of the Jacobian are given explicitly by

$$\lambda_{n,m} = \alpha + 2\beta(\cos(n\theta) + \cos(m\theta)) - \gamma(2\cos(n\theta) + 2\cos(m\theta) + 1)$$

if  $(n, m) \neq (0, 0)$ , and

$$\lambda_{0,0} = \alpha + 4\beta + (N^2 - 5)\gamma \quad (3)$$

where  $N$  is the lattice size. For the parameters used here,  $\lambda_{0,0}$  is the leading eigenvalue and thus Eq. (3) can be used to locate the deterministic bifurcation.

### 2.1.3. Vegetation turbidity model

We also demonstrate the DMD EWS methodology as applied to the vegetative turbidity model originally due to Ref. [21] which has been previously used as model for assessment of spatial EWS [8,13]. Briefly, the model is described by a system of coupled (lattice) ordinary differential equations using a finite-difference approximation to the diffusion operator as

$$\frac{dV_{i,j}}{dt} = r_v V_{i,j} \left( 1 - V_{i,j} \frac{h_E^p + E_{i,j}^p}{h_E^p} \right) + D (V_{i+1,j} + V_{i-1,j} + V_{i,j+1} + V_{i,j-1} - 4V_{i,j}) + \sigma dW_{i,j}$$

where

$$E_{i,j} = \frac{E_0 h_v}{h_v + V_{i,j}}.$$

Here  $V_{i,j}$  is the vegetation cover,  $r_v$  is the maximum vegetation growth rate,  $h_E$  is the half-saturation turbidity constant,  $h_v$  is the half-saturation vegetation constant,  $p$  is a Hill coefficient,  $D$  is the dispersion constant and  $\sigma$  is the standard deviation of the additive white noise. The parameter  $E_0$  represents the background turbidity is used here as the control parameter and assumed to increase linearly with time.

## 2.2. Dynamic mode decomposition

Here we provide a brief synopsis of the DMD algorithm so that readers unfamiliar with DMD may understand the broad outline. For more details the reader is referred to Refs. [15,16,22].

Consider an observation vector  $x_i$ , of length  $m$ , at  $t = i\Delta t$  from our dynamical system. (For the lung ventilation model this would be  $r$ , and for the vegetation turbidity model it is  $V$ . Also recall that we are using a lattice system so this observation vector is necessarily in reshaped form.) We define an observation window and then stack up the observations within window. For a window of size  $n$ , we have observations  $x_1, x_2, \dots, x_n$  arranged as the  $m$ -by- $n$  matrices [23]

$$\mathbf{X} = \begin{bmatrix} \downarrow & \downarrow & \dots & \downarrow \\ x_1 & x_2 & \dots & x_{n-1} \\ \uparrow & \uparrow & \dots & \uparrow \end{bmatrix} \quad (4)$$

and

$$\mathbf{X}' = \begin{bmatrix} \downarrow & \downarrow & \dots & \downarrow \\ x_2 & x_3 & \dots & x_n \\ \uparrow & \uparrow & \dots & \uparrow \end{bmatrix}. \quad (5)$$

Note the overlap between the two data matrices, such that  $\mathbf{X}'$  is shifted by  $\Delta t$  from  $\mathbf{X}$ . Thus we suppose that there exists an (unknown) linear operator  $A$  such that  $\mathbf{X}' = A\mathbf{X}$ , and thus  $A$  describes the advance in time of the observed snapshots. The goal of DMD is to obtain the eigendecomposition of  $A$ , but without forming  $A$  itself. This is done by first computing the singular value decomposition (SVD) of  $\mathbf{X} = \mathbf{U}\mathbf{\Sigma}\mathbf{V}^T$ , where in the usual way  $\mathbf{U}$  gives the left singular vectors,  $\mathbf{V}$  gives the right singular vectors, and  $\mathbf{\Sigma}$  is a diagonal matrix containing the singular values. We then form the square matrix  $\mathbf{S} = \mathbf{U}^T \mathbf{X}' \mathbf{V} \mathbf{\Sigma}^{-1}$  and compute its eigenvalues  $\lambda_j$  and eigenvectors  $\phi_j$ . The DMD eigenvalues are then given by  $\lambda_j$  and the DMD modes by  $\mathbf{U}\phi_j$ . For additional algorithmic and implementation details, including the usual implementation as a for-loop, the reader is referred to [22].

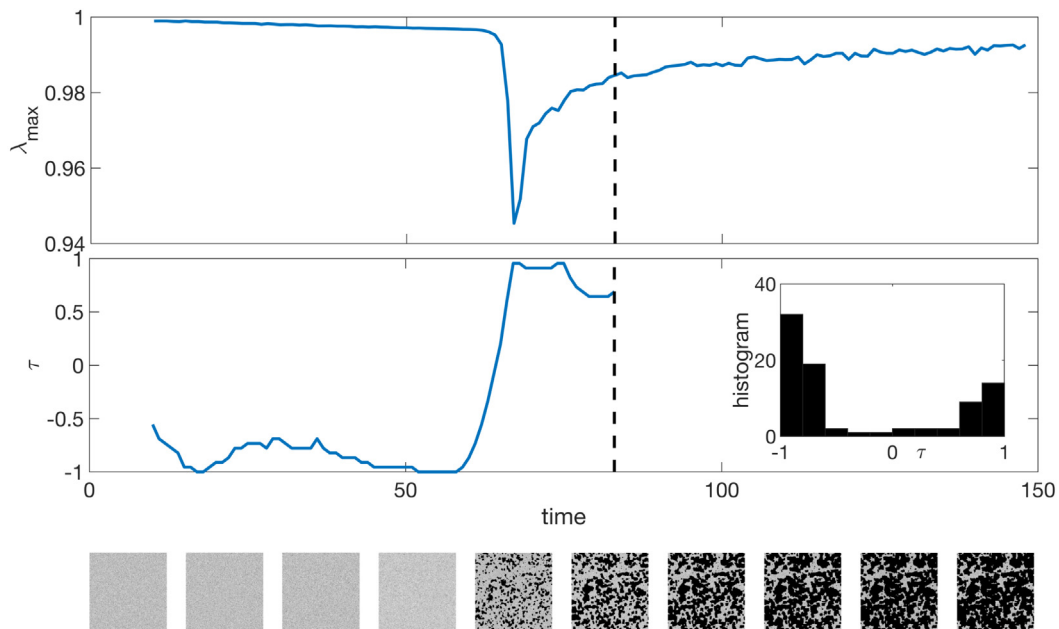


**Fig. 1.** Single realization of the model and proposed spatial EWS. Upper panel:  $\lambda_{max}$ ; middle panel: Kendall's  $\tau$ ; lower panel(s): system evolution snapshots displaying emergence of spatial structure. Here the DMD sliding window size is taken to be 10 timesteps.

### 2.3. Proposed spatial EWS using DMD

Our proposed method of spatial EWS uses a sliding window of size  $n$  observations. For each set of  $n$  observations, DMD is performed as described above. We then take the leading DMD eigenvalue  $|\lambda_{max}|$ , which itself is time varying as the sliding window advances, as our EWS. The effectiveness of this potential signal is assessed in the usual way by calculating Kendall's  $\tau$  (rank correlation coefficient) between the signal  $|\lambda_{max}|$  and the control parameter prior to the underlying bifurcation. Note that here we know the underlying control parameters ( $\kappa$  for the lung ventilation model and  $E_0$  for the vegetation turbidity model); they are ramped linearly in time and used both for simulating the synthetic snapshot data and also for purposes of computing the Kendall's  $\tau$  correlations. In practice, however, the underlying control coefficient would be unknown. For purposes of quantitative assessment, Kendall correlation ( $|\tau|$ ) coefficients close to 1 are generally interpreted as providing good predictive value as an EWS, though care should be taken [24].

## 3. Results

A single realization of the lung ventilation model and proposed spatial EWS is shown in Fig. 1. The upper panel shows the proposed EWS  $\lambda_{max}$  versus time. The middle panel shows Kendall's  $\tau$ , with the histogram in the inset. The lower panels show a subset of the system evolution snapshots and demonstrate the emergence of the spatially-structured solution. The vertical dashed line indicates the time when the control parameter reaches the deterministic bifurcation. Together these suggest that the leading DMD eigenvalue may provide a useful spatial EWS, with good correlation ( $|\tau| \sim 1$ ) preceding the tipping point, at least in this example.

We also apply the same DMD EWS methodology to the vegetation turbidity model, using the parameter values  $h_E = 2$ ,  $r_v = 0.5$ ,  $h_v = 0.2$ ,  $p = 4$ ,  $D = 0.9$ ,  $\sigma = 0.02$  and ramping  $E_0$  linearly from 6 to 7.5, shown in Fig. 2. As with the lung ventilation model, the leading DMD eigenvalue shows good potential as a leading indicator of the tipping point as indicated by the  $\tau$  criterion.

While these single realizations show promise, a more robust examination requires repeated trials, as well as the varying temporal resolution of the underlying signal, the sliding window size, and the noise level. Fig. 3 shows the contours of the mode of the Kendall's  $\tau$  distribution in the period preceding the tipping point, as the observation timestep and sliding window size are varied. The three panels show noise levels 0.05, 0.1 and 0.2 (from left to right). This suggests that for a reasonably broad range of observation frequency and window size, the DMD leading eigenvalue can potentially provide a valuable EWS. Unsurprisingly, the range over which  $|\tau| \sim 1$ , and thus  $\lambda_{max}$  is a worthwhile EWS, is larger for lower noise levels. A more explicit comparison of the modes associated with these leading eigenvalues is also instructive; as shown in Fig. 4 these reconstruct the spatial changes seen in the underlying system, as designed.

It is also worth considering further the details of the DMD reconstruction as we vary both the observation timestep and the sliding window size. Clearly, these numerical parameters interact with the intrinsic timescale of the dynamics of

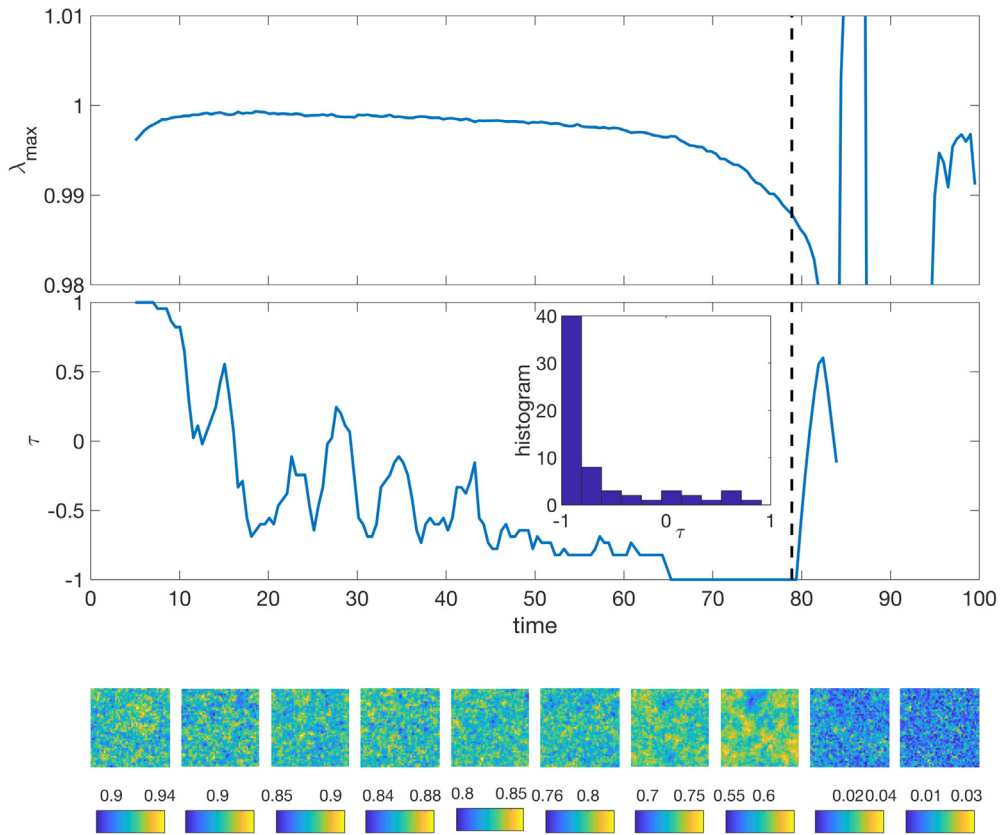


**Fig. 2.** Single realization of the vegetative turbidity model and proposed spatial EWS. Upper panel:  $\lambda_{max}$ ; middle panel: Kendall's  $\tau$ ; lower panel(s): system evolution snapshots displaying emergence of spatial structure. The vertical range of the upper panel is chosen to show the behaviour prior to the tipping point. Here the DMD sliding window size is taken to be 10 timesteps.

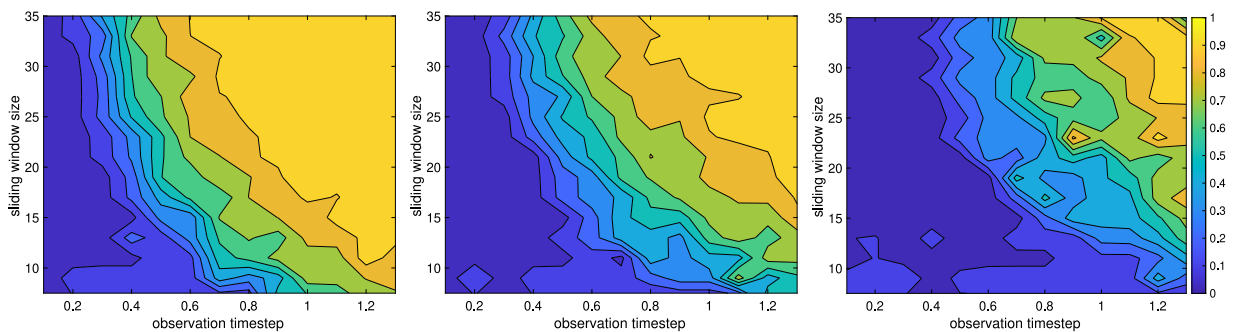


**Fig. 3.** Contours of the absolute value of the mode of the Kendall's  $\tau$  distribution as temporal resolution of the underlying signal, sliding window size, and the noise level are varied. The three panels show noise levels 0.05, 0.1 and 0.2 (from left to right).

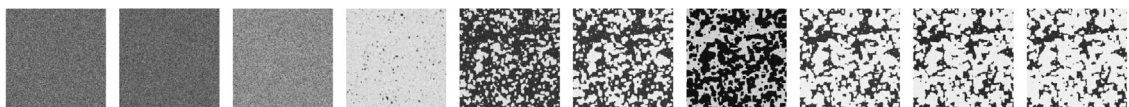


**Fig. 4.** DMD leading modes corresponding to the simulation in Fig. 1.

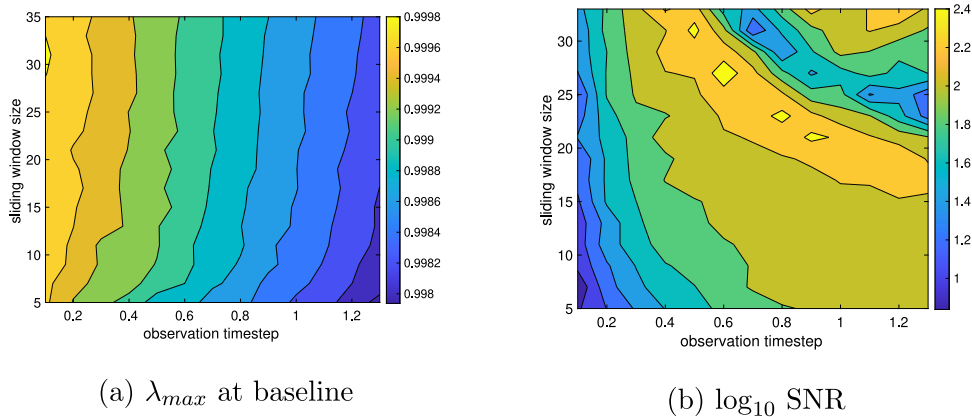


**Fig. 5.** Stability of the leading DMD eigenvalue in the lung ventilation model as the observation timestep and sliding window size are varied. The signal-to-noise ratio (SNR) is defined here as the change  $\lambda_{max}$  between baseline and the tipping point, divided by the standard deviation of the observations near baseline.

the underlying system. Because it may not be possible, in practice, to know the underlying timescale precisely *a priori*, it is useful to assess the sensitivity of the method to these parameters. To this end, we show also the stability of the leading eigenvalue and the overall signal-to-noise ratio in Fig. 5. This indicates that overall SNR is relatively robust to the numerical parameters, and that these need not be tuned particularly closely to the underlying timescale.

It is also instructive to compare with so-called “generic” EWS indicators (for non-spatial systems) applied to the spatial mean of the system; Fig. 6 shows autoregression, autocorrelation, standard deviation and skewness, all computed with Gaussian detrending [25]. For this particular system, based on the  $\tau$  histograms, both the standard deviation and skewness may provide useful EWS, as expected for a transition arising from a fold bifurcation [4]. Knowing this *a priori*, however, requires a degree of non-generic analysis in order to anticipate which indicators may be valuable from those which are not. In contrast, autoregression and autocorrelation are not particularly informative for this system.

#### 4. Discussion

Early warning signals of tipping points in low-dimensional systems have evolved from largely empirical, ad hoc beginnings to the point where there is now a reasonably well-developed theory underpinning their efficacy. For example, B-tipping can now be characterized for different types of underlying bifurcation [4]. Spatial EWS, on the other hand, are still in their relative infancy; several indicators have been proposed, such as spatial correlation [8], spatial variance, spatial skewness [9] and the discrete Fourier transform [10]. Here we propose to add the DMD leading eigenvalue as a viable candidate as a spatial EWS, based on the idea of critical slowing down in the leading mode, and its promise in these representative synthetic datasets.

Spatial EWS would also benefit from a firmer theoretical foundation in the spirit of their non-spatial cousins. Some work in this direction has recently appeared regarding the eigenvalues of the covariance matrix [13], and we have leveraged this idea by attempting to capture the mode itself more directly using DMD rather than indirectly via the eigenvalues of the covariance matrix. However, the theoretical tools which served so well for low-dimensional systems are not readily applied to spatial systems and much remains to be done. Additionally, it may prove useful to make use of the leading mode itself, rather than only its associated eigenvalue, or perhaps secondary modes as well, rather than simply the leading eigenvalue as we have done here. A more robust theory will also encapsulate a broader class of spatial tipping points, rather than being confined to specific (if representative) models. The potential EWS value of the leading dynamic mode may help to develop this theory.

One aspect of DMD which is relevant to its application as a spatial EWS is that it is particularly adept at reconstructing periodic systems. However, the models used here are not of this type (the ventilation model has already been averaged over tidal breathing.) However, despite the fact that DMD may not provide a particularly good system reconstruction in this environment, the leading mode eigenvalue is still a good predictor; that may be because we do not require a full reconstruction, but only a quantification of the critical slowing down in the leading mode. As shown in Fig. 5, the baseline values of  $\lambda_{max}$  are reasonably stable with respect to the observational parameters, and despite the relatively small scale of changes in  $\lambda_{max}$ , the overall signal-to-noise ratio is favourable. We also note that it is possible to optimize the DMD procedure to minimize the effects of additive noise [26]. We have not employed the optimized version here, but this would likely further improve the SNR (and hence potential usefulness of the EWS).

Although a majority of EWS and tipping point study has been conducted with an emphasis towards applications in climate or ecology, physiology may be a discipline in which this theory will also thrive. The reasons for this are twofold: first, that physiological systems do appear to exhibit tipping points and there is predictive value in EWS in this context [2],

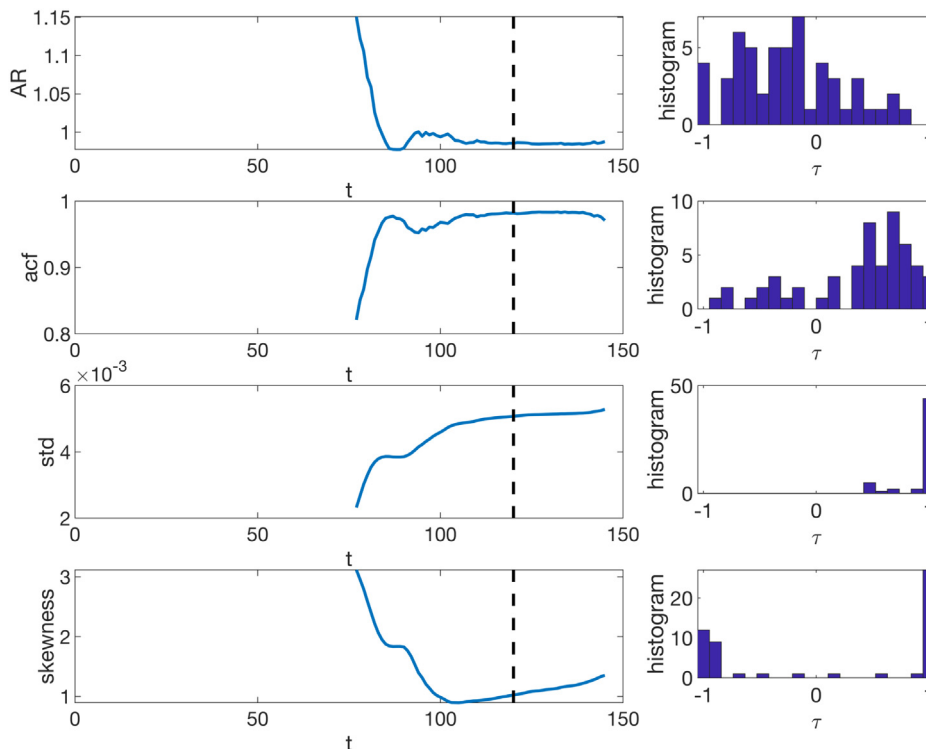


**Fig. 6.** Comparison with generic EWS; autoregression, autocorrelation, standard deviation and skewness, all computed with Gaussian detrending [25]. Here the ramping of the control parameter has been slowed, relative to previous simulations, to allow time for the detrending to establish before the (deterministic) bifurcation is reached.

and in future such studies could benefit from a *a priori* study of the EWS indicators (for example, arising from a particular bifurcation structure), rather than relying on generic methods. Secondly, applications in physiology offer a potentially rich data source, with each patient offering, in essence, an independent sample. Thus while study of tipping points may help to further our understanding of physiology, physiology may in turn contribute the data to further our study of tipping points.

### CRediT authorship contribution statement

**G.M. Donovan:** Conceptualization, Methodology, Software, Validation, Formal Analysis, Investigation, Writing. **C. Brand:** Methodology, Writing – review & editing.

### Declaration of competing interest

The authors declare that they have no known competing financial interests or personal relationships that could have appeared to influence the work reported in this paper.

### Appendix. Simplification of lung-ventilation model

The lung ventilation model used in this paper is a simplified version of the model first described in [20]. The changes are twofold. First, the empirical airway pressure–radius relationship (i.e. Eq. 2 in Ref. [20]), which describes the highly nonlinear opening and closing process of the airway and was first described by Lambert et al. [27] as matched rectangular hyperbolae, is replaced by a three-parameter sigmoidal approximation of the form  $R(P) = \frac{R_{ref}}{1 + \exp(-c(P - P_l))}$  where  $R_{ref}$  is the reference radius (as in Ref. [20]),  $c = 0.725 \text{ cm H}_2\text{O}^{-1}$  and  $P_l = 1.33 \text{ cm H}_2\text{O}$ . The parameters  $R_{ref}$ ,  $c$  and  $P_l$  were optimized using the python `scipy.optimize` curve-fit function to fit the airway radius function from Ref. [20].

Secondly, the variables and parameters were non-dimensionalized and simplified as follows:  $\hat{r}_i = \frac{r_i}{R_{ref}}$ ,  $\hat{t} = \rho t$ ,  $\hat{P}_b(0) = cP_b(0)$ ,  $\hat{P}_l = cP_l$ ,  $\hat{A} = \frac{A}{5} R_{ref}^4$ ,  $\hat{k} = \frac{\kappa}{21.4 \text{ cm H}_2\text{O}}$  and  $k = 14.065$ . Finally, we drop the hats from the non-dimensionalized quantities to obtain the four-parameter non-dimensional model given in Eqs. (1) and (2).

## References

- [1] T.M. Lenton, J. Rockström, O. Gaffney, S. Rahmstorf, K. Richardson, W. Steffen, H.J. Schellnhuber, *Nature* (2019).
- [2] U. Frey, T. Brodbeck, A. Majumdar, D.R. Taylor, G.I. Town, M. Silverman, B. Suki, *Nature* 438 (2005) 667.
- [3] P. Ashwin, S. Wiczorek, R. Vitolo, P. Cox, *Phil. Trans. R. Soc. A* 370 (2012) 1166.
- [4] C. Kuehn, *Physica D* 240 (2011) 1020.
- [5] V. Dakos, E.H. Van Nes, P. d'Odorico, M. Scheffer, *Ecology* 93 (2012a) 264.
- [6] T. Lenton, V. Livina, V. Dakos, E. Van Nes, M. Scheffer, *Phil. Trans. R. Soc. A* 370 (2012) 1185.
- [7] J.M.T. Thompson, J. Sieber, *Int. J. Bifurcation Chaos* 21 (2011) 399.
- [8] V. Dakos, E.H. van Nes, R. Donangelo, H. Fort, M. Scheffer, *Theor. Ecol.* 3 (2010) 163.
- [9] V. Guttal, C. Jayaprakash, *Theor. Ecol.* 2 (2009) 3.
- [10] S. Carpenter, W. Brock, *Ecosphere* 1 (2010) 1.
- [11] S. Kéfi, V. Guttal, W.A. Brock, S.R. Carpenter, A.M. Ellison, V.N. Livina, D.A. Seekell, M. Scheffer, E.H. van Nes, V. Dakos, *PLoS One* 9 (2014) e92097.
- [12] V. Dakos, S. Kéfi, M. Rietkerk, E.H. Van Nes, M. Scheffer, *Amer. Nat.* 177 (2011) E153.
- [13] S. Chen, E.B. O'Dea, J.M. Drake, B.I. Epureanu, *Sci. Rep.* 9 (2019).
- [14] P.J. Schmid, *J. Fluid Mech.* 656 (2010) 5.
- [15] J.H. Tu, C.W. Rowley, D.M. Luchtenburg, S.L. Brunton, J.N. Kutz, *J. Comput. Dyn.* 1 (2014) 391.
- [16] J.N. Kutz, S.L. Brunton, B.W. Brunton, J.L. Proctor, *Dynamic Mode Decomposition: Data-Driven Modeling of Complex Systems*, SIAM, 2016.
- [17] B.W. Brunton, L.A. Johnson, J.G. Ojemann, J.N. Kutz, *J. Neurosci. Methods* 258 (2016) 1.
- [18] H. Lange, S.L. Brunton, J.N. Kutz, *J. Mach. Learn. Res.* 22 (2021) 1.
- [19] The connection between DMD and the discrete Fourier transform can be made explicit under certain conditions [28].
- [20] G.M. Donovan, T. Kritter, *J. Math. Biol.* 70 (2015) 1119.
- [21] M. Scheffer others, *Ecology of Shallow Lakes*, Vol. 1, Springer, 1998.
- [22] S.L. Brunton, J.N. Kutz, *Data-Driven Science and Engineering: Machine Learning, Dynamical Systems, and Control*, Cambridge University Press, 2019.
- [23] Sometimes denoted  $V_1$  and  $V_2$  rather than  $X$  and  $X'$ .
- [24] S. Chen, A. Ghadami, B.I. Epureanu, *arXiv preprint arXiv:2010.02478* 2020.
- [25] V. Dakos, S.R. Carpenter, W.A. Brock, A.M. Ellison, V. Guttal, A.R. Ives, S. Kéfi, V. Livina, D.A. Seekell, E.H. van Nes, et al., *PLoS One* 7 (2012b) e41010.
- [26] T. Askham, J.N. Kutz, *SIAM J. Appl. Dyn. Syst.* 17 (2018) 380.
- [27] R.K. Lambert, T.A. Wilson, R.E. Hyatt, J.R. Rodarte, *J. Appl. Physiol.* 52 (1982) 44.
- [28] K.K. Chen, J.H. Tu, C.W. Rowley, *J. Nonlinear Sci.* 22 (2012) 887.